Proceedings World Geothermal Congress 2026
Calgary, Canada, June 8 – 11, 2026

Geothermal Exploration in Western Canada Using Magnetotelluric Data

Cedar Hanneson[1]*, Martyn Unsworth[2], James Craven[3],
Victoria Tschirhart[3], Stephen Grasby[3] and Maurice Colpron[4]
Athabasca University[1]*, University of Alberta[2], Geological Survey of Canada[3], Yukon Geological Survey[4]
* corresponding author, channeson@athabascau.ca

Keywords: British Columbia, Yukon, electrical conductivity, electrical resistivity, geophysics, magnetotellurics

ABSTRACT

Magnetotelluric data were used to image subsurface electrical resistivity in three study areas in western Canada: (1) Mount Meager, British Columbia, (2) Whitehorse, Yukon, and (3) Haines Junction, Yukon. The Mount Meager model imaged geothermal caprocks beneath Pylon Peak and Fish Creek, a magma body at 5–15 km below sea level, and fluid pathways from this magma body to the surface near an active fumarole. The Whitehorse model imaged a dipping conductor below Takhini Hot Springs, likely correlated with a fault zone, allowing geothermal fluids to ascend from depth. The Haines Junction model imaged a dipping conductor near the Shakwak fault and another just west of the village, possibly correlated with fluid flow in the upper crust.

1 INTRODUCTION

The Canadian Cordillera in western Canada is an accretionary orogen and it is often divided into five geomorphological belts: the Insular, Coast, Intermontane, Omineca, and Foreland belts, listed from west to east (Gabrielse et al., 1991). The three study areas in British Columbia (BC) and Yukon are within the Coast and Intermontane belts. The Coast belt encompasses the high-elevation, extensively glaciated mountain range that runs the length of western BC and is dominantly made up of large Mesozoic-Cenozoic plutonic complexes. Modern continental arc volcanoes associated with the Cascadia subduction zone have developed on top of the plutonic complex. The Intermontane belt is an elevated plateau with subdued relief and is dominantly made up of early Mesozoic island arc volcanic rocks and associated sedimentary sequences. Mount Meager, BC and Haines Junction, Yukon are in the Coast belt, and Whitehorse, Yukon is in the Intermontane belt (Figure 1).

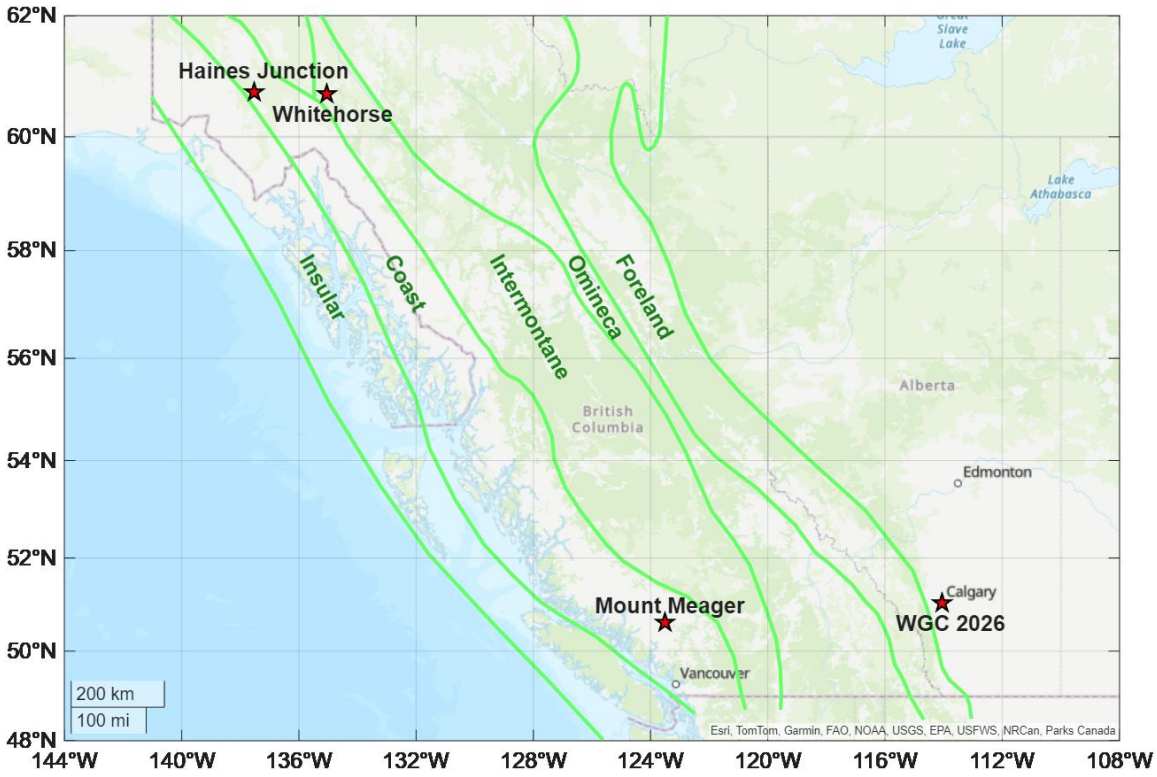


Figure 1. Map of western Canada with the locations of our study areas in British Columbia (BC) and Yukon. Geomorphological belts are shown in green.

Western Canada has significant, yet currently unexploited, geothermal resources (Grasby et al., 2012). The total geothermal power potential in BC and Yukon has been estimated at 3,000–5,000 MWe (Ghomshei, 2010). Electrical resistivity is a useful physical property to measure during geothermal exploration because it is sensitive to the presence of fluids such as brines and partially molten rocks, as well as clay minerals formed by hydrothermal alteration. These substances have low electrical resistivity, compared with dry, unaltered rocks (Muñoz, 2014).

The magnetotelluric (MT) method is a passive source electromagnetic (EM) geophysical method used to image subsurface electrical resistivity. It uses naturally occurring radio waves as the source and frequency as a proxy for depth. High frequencies are measured in the audiomagnetotelluric (AMT) band, and they are used to image shallow structures. Lower frequencies are used in broadband magnetotelluric (BBMT) data collection, and they can image structures throughout the crust.

BBMT data were collected near Mount Meager, BC, in 2019–2020. They were used to image the magmatic and geothermal systems beneath this Holocene volcanic centre. AMT and BBMT data were collected in southwestern Yukon in 2021–2023. AMT data measured near Haines Junction were used to image the uppermost 3 km of the subsurface. BBMT data measured near Whitehorse were used to image the upper 30 km.

2 GEOLOGICAL OVERVIEW

2.1 Mount Meager (Q̓welq̓welústen)

The Garibaldi Volcanic Belt (GVB) at the northern end of the Cascadia subduction zone is a Quaternary glaciovolcanic arc extending from northern Washington into southwestern BC (Venugopal et al., 2020). The GVB includes the Mount Meager volcanic complex (MMVC), an active calc-alkaline volcanic complex which has had at least two recent explosive volcanic eruptions, ~2,400 and ~24,300 years ago (Hickson, 1994; Russell et al., 2021). The study area surrounds the MMVC (Figure 2).

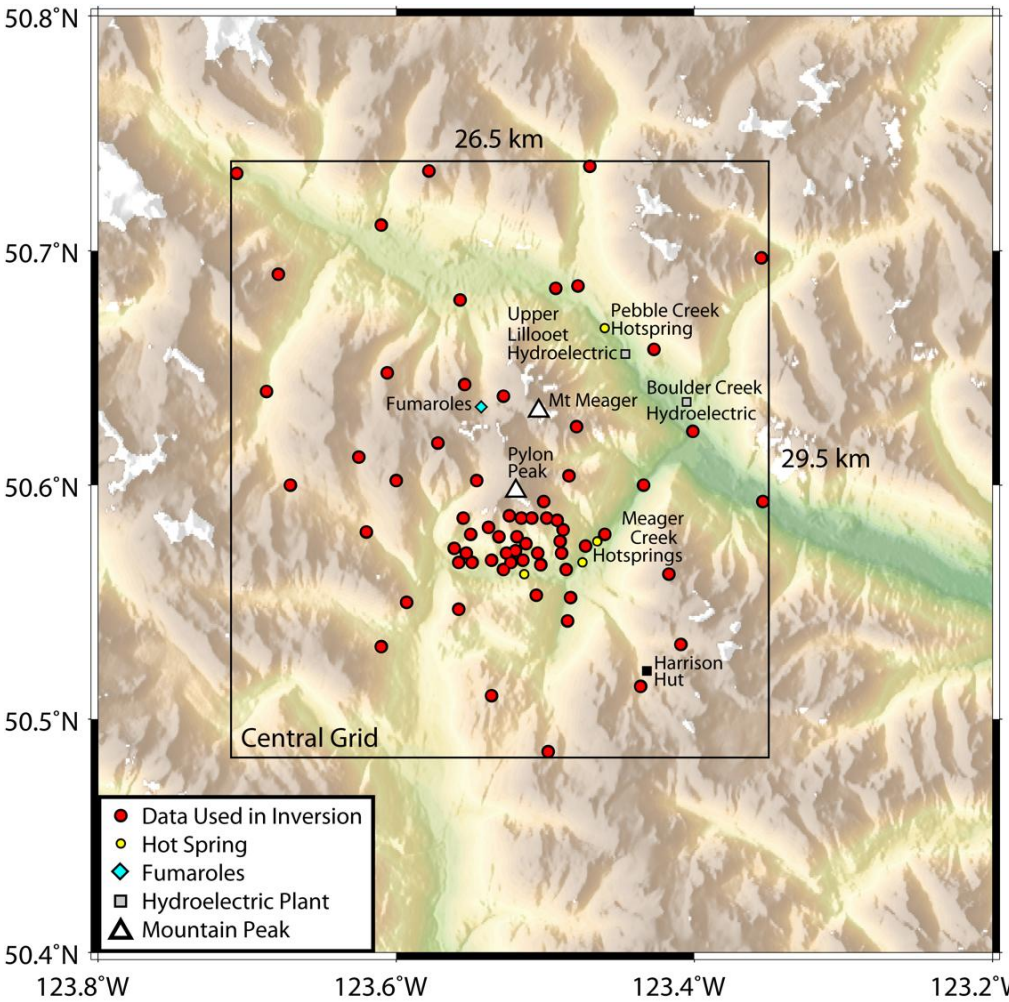


Figure 2. Topographic map of the Mount Meager region. Red circles are MT station locations, yellow circles are hot spring locations, and the blue diamond is the fumarole location. (Hanneson and Unsworth, 2023)

The MMVC includes basaltic rocks of the Cracked Mountain Assemblage and Mosaic Assemblage, andesitic-to-dacitic rocks of the Plinth Assemblage and Capricorn Assemblage, and dacitic rocks of the Plinth Pyroclastic Deposit and Pebble Creek Formation (PCF; Harris et al., 2022; Read, 1990; Russell et al., 2021). This 400 ka eruptive history follows a trend of increasing silica content. The youngest rocks (2370 ± 50 years old) of the MMVC belong to the PCF. The alkali-silica content of these rocks places them near the dacite–trachydacite boundary, with some samples near the rhyolite boundary (Harris et al., 2022; Russell et al., 2021; Stasiuk et al., 1996).

2.2 Whitehorse

Whitehorse is the capital of Yukon and largest city in northern Canada. The Whitehorse batholith is mid-Cretaceous granodiorite and quartz diorite; the Mandanna member of the Aksala formation is Upper Triassic greywacke, pebble conglomerate, and mudstone; the Hancock member of the Aksala formation is Upper Triassic massive to thick-bedded limestone (Yukon Geological Survey, 2024). The former is located near Whitehorse and the latter two are near Takhini Hot Springs, located 24 km northwest of Whitehorse (Figure 3).

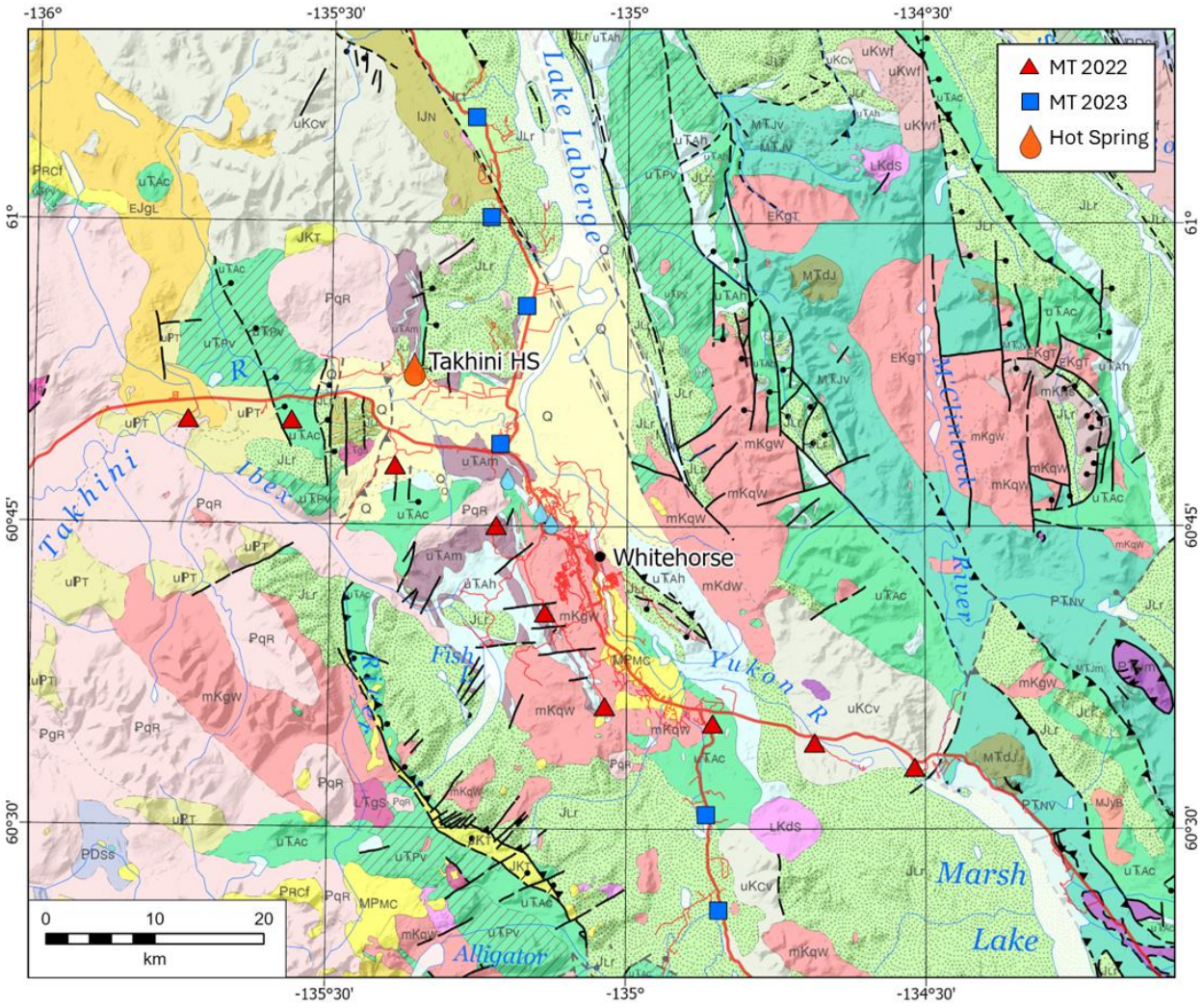


Figure 3. Bedrock geology map of the Whitehorse region (Yukon Geological Survey, 2024). Red triangles and blue squares are MT station locations from 2022 and 2023, respectively. Whitehorse batholith = mKgW. Mandanna member of the Aksala formation = uTAm. Hancock member of the Aksala formation = uTAh.

2.3 Haines Junction

Haines Junction is a village situated at the junction between the Alaska Highway (also known as Yukon Highway #1) and Haines Road (also known as Yukon Highway #3) as shown in Figure 4. It is located 130 km west of Whitehorse, east of the Saint Elias Mountains, and just north of a braided river named the Dezadeash River.

Haines Junction is located above the Late Triassic Bear Creek assemblage, which is characterized by metavolcanic rocks overlying metasedimentary rocks, with some interlayering in the upper sequence (Israel et al., 2015). The volcanic rocks are predominantly andesitic to basaltic in composition, and the sedimentary rocks are mostly sandstone, siltstone, and mudstone, including some graphitic phyllite (Israel et al., 2015).

The northeastern part of the study area is occupied by the Kluane Schist, which is separated from the Bear Creek assemblage by the Shakwak fault (Figure 4). The Kluane Schist is composed primarily of quartz-mica schist (Israel et al., 2011). Intruding the Kluane Schist and Bear Creek assemblage, and cutting the Shakwak fault, is a felsic pluton of the Hayden Lake suite (Colpron et al., 2016).

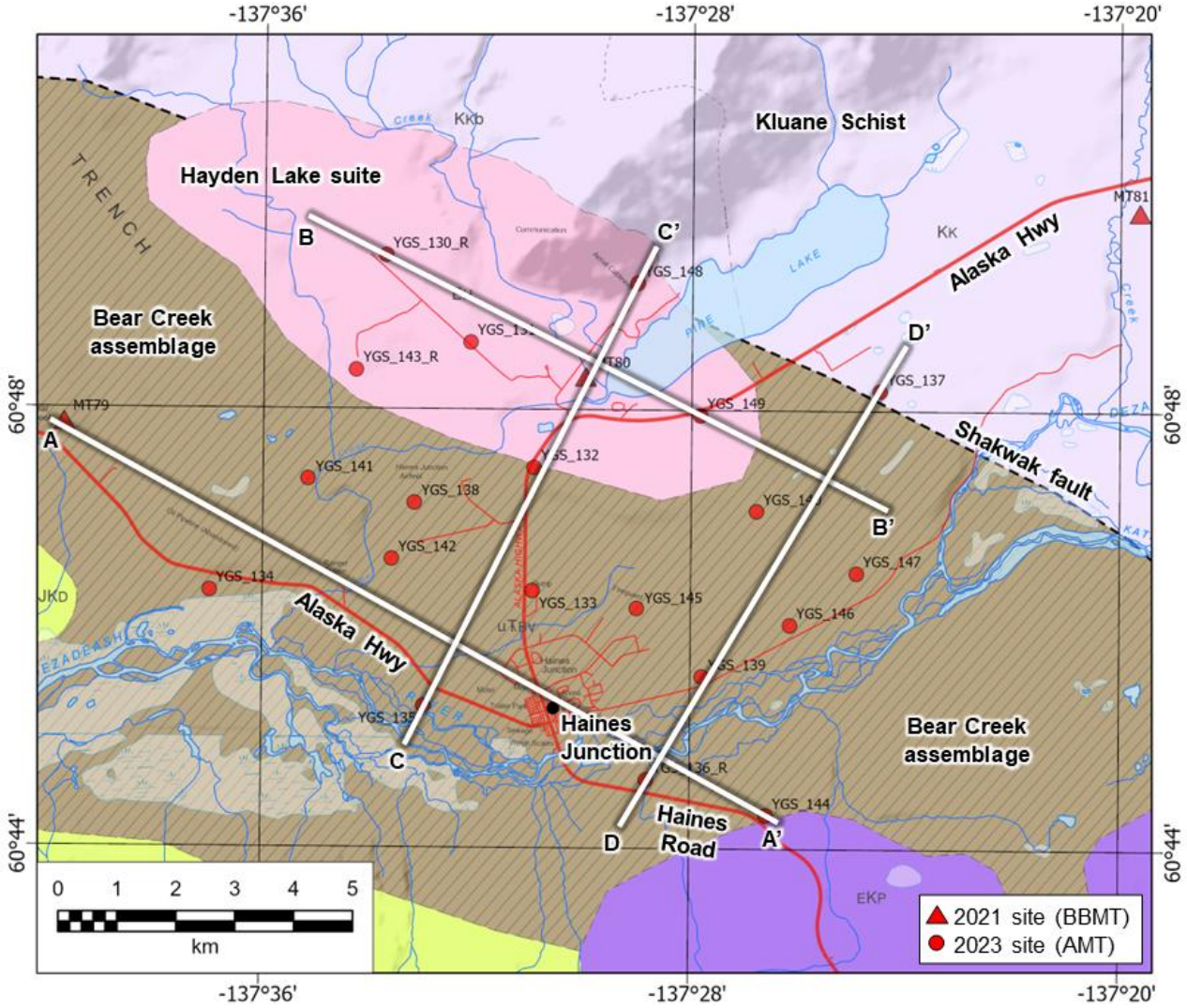


Figure 4. Bedrock geology map of the Haines Junction region (Yukon Geological Survey, 2024). Red circles and triangles are MT station locations. White lines indicate locations of cross-sections shown in Figure 10.

3 DATA AND METHODS

In each of our three studies, we ran multiple inversions to test a sufficiently large range of model parameters and inversion parameters. The preferred 3-D resistivity models for Mount Meager, Haines Junction, and Whitehorse were chosen after the completion of 27, 18, and 14 inversions, respectively, each of which included many iterations. The ModEM inversion algorithm of Kelbert et al. (2014) was used in all cases.

The model covariance length scale is a measure of model smoothness and higher values correspond to more smoothing applied across cell boundaries. The effect of varying the covariance length scale was investigated by running inversions with covariance length scale values of 0.2, 0.3, 0.4 and 0.5 for each of the three study areas, while keeping all other inversion parameters identical. Based on the results of these tests, a value of 0.4 was chosen as the preferred model covariance length scale for each of the three study areas.

Another measure of model smoothness is the regularization parameter, λ. Higher values of λ result in resistivity models that are more spatially smooth, with higher data misfit. Conversely, lower values of λ result in resistivity models that are less spatially smooth, with lower data misfit. We investigated the effect of starting the inversion with either $\lambda = 10$ or $\lambda = 1$, while keeping all other inversion parameters identical. In each case, λ was decreased by a factor of 10 each time the change in misfit between successive iterations was less than 0.0001 until a value of $\lambda < 10^{-8}$ was reached, then the inversion was terminated.

There is a trade-off between minimizing the model norm, a measure of model roughness, and minimizing the root-mean-square (R.M.S.) data misfit. By looking at L-curves and visually comparing a range of resistivity models, a preferred model for each study area was chosen, as described in the following three subsections.

3.1 Mount Meager (Q̓welq̓welústen)

The data and methods used at Mount Meager were described in detail by Hanneson and Unsworth (2023). Impedance and tipper data collected at 66 BBMT sites were inverted using a set of 29 frequencies in the range 1 mHz – 400 Hz. The preferred resistivity model is from iteration 323 of an inversion starting with $\lambda = 10$, and λ had decreased to a value of 10^{-6} at this point. This model has an R.M.S. misfit of 1.92 and the individual misfit of each MT site is shown in Figure 5. The starting model was a halfspace with a resistivity of 100 Ωm and a misfit of 11.7. The horizontal resolution is 250 m, and topography is included with a vertical discretization of 50 m.

3.2 Whitehorse

Impedance and tipper data collected at 15 BBMT sites were inverted using a set of 24 frequencies in the range 0.31 mHz – 430 Hz. The preferred resistivity model is from iteration 169 of an inversion starting with $\lambda = 10$, and λ had decreased to a value of 1 at this point. This model has an R.M.S. misfit of 1.88 and the individual misfit of each MT site is shown in Figure 6. The starting model was a halfspace with a resistivity of 100 Ωm and a misfit of 13.1. The horizontal resolution is 1 km, and topography is included with a vertical discretization of 50 m.

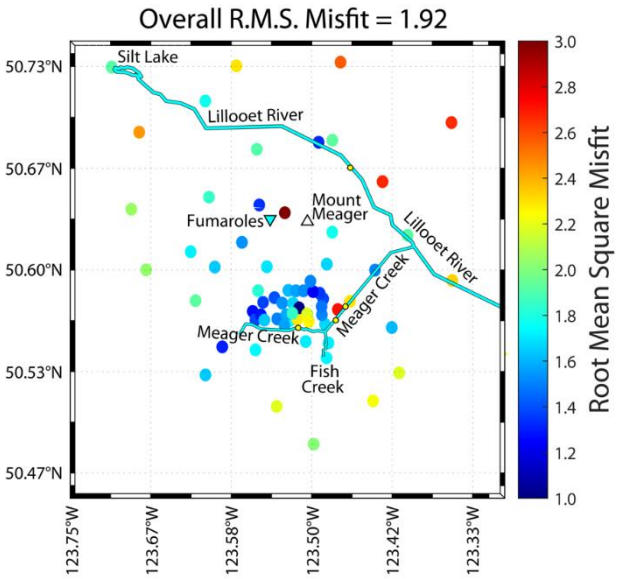


Figure 5. Root-mean-square misfit of each MT site near Mount Meager, BC. The overall misfit is 1.92. (Hanneson and Unsworth, 2023)

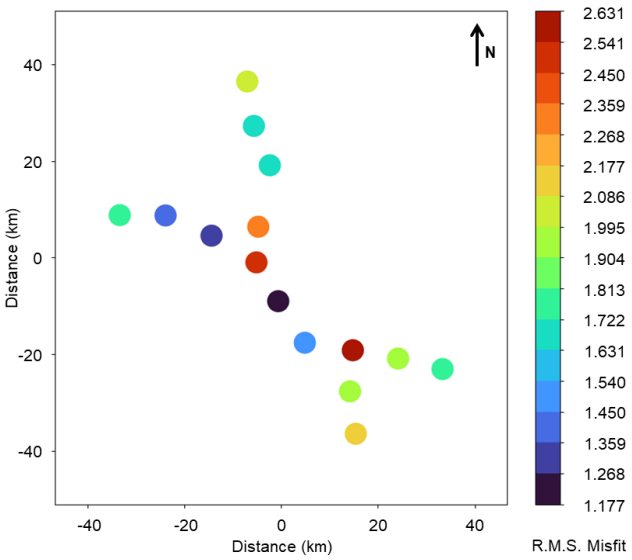


Figure 6. Root-mean-square misfit of each MT site near Whitehorse, Yukon. The overall misfit is 1.88. Distance is relative to the centre of the model.

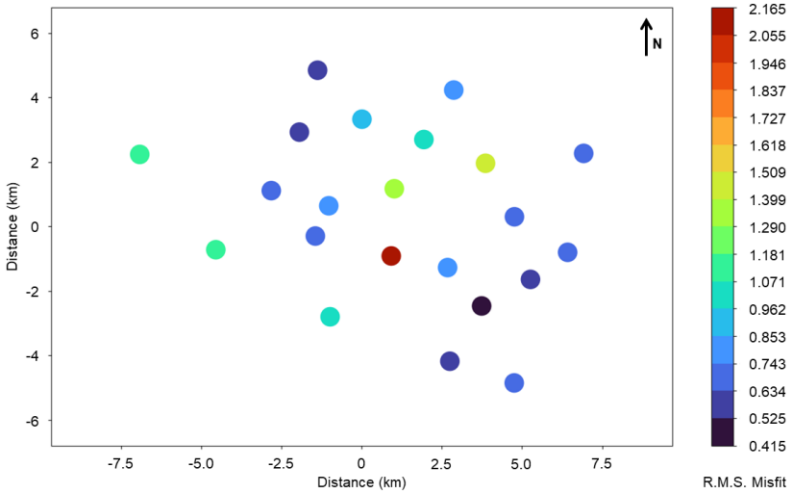


Figure 7. Root-mean-square misfit of each MT site near Haines Junction, Yukon. The overall misfit is 0.954. Distance is relative to the centre of the resistivity model.

3.3 Haines Junction

Impedance and tipper data collected at 20 AMT sites and two BBMT sites were inverted using a set of 20 frequencies in the range 3.7 Hz – 10 kHz. The preferred resistivity model is from iteration 107 of an inversion starting with $\lambda = 1$, and λ had decreased to a value of 0.001 at this point. This model has an R.M.S. misfit of 0.95 and the individual misfit of each MT site is shown in Figure 7. The starting model was a halfspace with a resistivity of 316 Ωm and a misfit of 9.07. The horizontal resolution is 125 m, and topography is included with a vertical discretization of 25 m.

4 RESISTIVITY MODELS

4.1 Mount Meager (Q̓welq̓welústen)

The preferred 3-D resistivity model for Mount Meager is presented in Figure 8. The upper 6–7 km are generally resistive, with a number of small near surface conductors. These conductors are located in the central part of the model, near Mount Meager and Meager Creek. Specifically, there are significant conductors in the upper 2 km beneath Pylon Peak and Fish Creek. These conductors were interpreted as low-permeability, clay-rich layers, acting as caprocks to geothermal fluids below (Hanneson and Unsworth, 2023), consistent with the results of Hormozzade Ghalati et al. (2022).

Below the resistive upper crust, there is a large conductor in the depth range 5–15 km below sea level. It has a resistivity of 0.3–30 Ωm and an average resistivity of ~3 Ωm. Above the northern part of this deep conductor, there is a conductive zone extending up toward Mount Meager and the fumaroles; it has a resistivity of 20–90 Ωm. The deep conductor was interpreted as a magma body containing 18–32% dacitic-to-trachydacitic melt with 6–8 wt.% H_2O at a temperature in the range 800–900 °C, and the conductive zone above it was interpreted as hydrothermal alteration minerals along fluid pathways from a degassing magma body to the surface (Hanneson and Unsworth, 2023).

4.2 Whitehorse

The preferred 3-D resistivity model for the Whitehorse region is presented in Figure 9. There is a zone of high resistivity extending to a depth of ~15 km, southwest of Whitehorse, interpreted as the Whitehorse batholith. There is a conductor that surfaces just south of Takhini Hot Springs and extends into the middle crust, to a depth of 15 km or more. The base of the conductor dips ~50° to the south, beneath Takhini Hot Springs. This could represent a deep fault that facilitates the transport of hot fluids to the surface.

Takhini Hot Springs occur near the geologic contact between the Mandanna sandstone and the Hancock limestone, as do four warm springs in the region (Witter, 2025). Near the surface, the dipping boundary between high and low resistivity (black dashed lines in Figure 9) could correspond to the boundary between these two rock units, with conductive sandstone above and resistive limestone below. However, this contact is unlikely to extend into the middle crust. Geothermal research in the Whitehorse region is ongoing and further interpretations are forthcoming.

4.3 Haines Junction

The preferred 3-D resistivity model for Haines Junction is presented in Figure 10. Cross-section A-A' shows low resistivity (less than 200 Ωm) beneath Haines Junction. Cross-sections B-B' and C-C' show a clear resistivity contrast between the plutonic Hayden Lake suite (higher resistivity) and the metamorphic Bear Creek assemblage (lower resistivity). Cross-section D-D' shows high resistivity (~1,000 Ωm) below MT station YGS_137, suggesting that the Kluane Schist is less graphitic in this area, near the edge of the unit, or that the graphite is not interconnected.

The shallow conductor associated with the Bear Creek assemblage dips steeply to the southwest, below and southwest of YGS_137. This could be an electrical expression of the Shakwak fault at depth. If so, it could provide a pathway for fluids to ascend from depth. A similar resistivity pattern is observed near MT station YGS_135, which is ~1.3 km west of a well with a water temperature of ~17 °C at a depth of ~370 m and a ground surface temperature of 2–4 °C (EBA Engineering, 2003). This gives an estimated geothermal gradient of 35–40 °C/km. Geothermal research in the Haines Junction area is ongoing and further interpretations are forthcoming.

5 CONCLUSIONS

BBMT data were used to image the upper 25–30 km of the subsurface near Mount Meager, BC, and Whitehorse, Yukon; and AMT data were used to image the upper 2–3 km near Haines Junction, Yukon. The Mount Meager model imaged geothermal caprocks within the upper 2 km, a magma body at 5–15 km below sea level, and fluid

pathways from this magma body to the surface near active fumaroles. The Yukon models imaged dipping conductors near Takhini Hot Springs, Haines Junction, and the Shakwak fault. These dipping boundaries between high and low resistivity could correspond to boundaries between different rock units and/or fault zones allowing geothermal fluids to ascend from depth. Geothermal research in southwestern Yukon is ongoing and further interpretations are forthcoming.

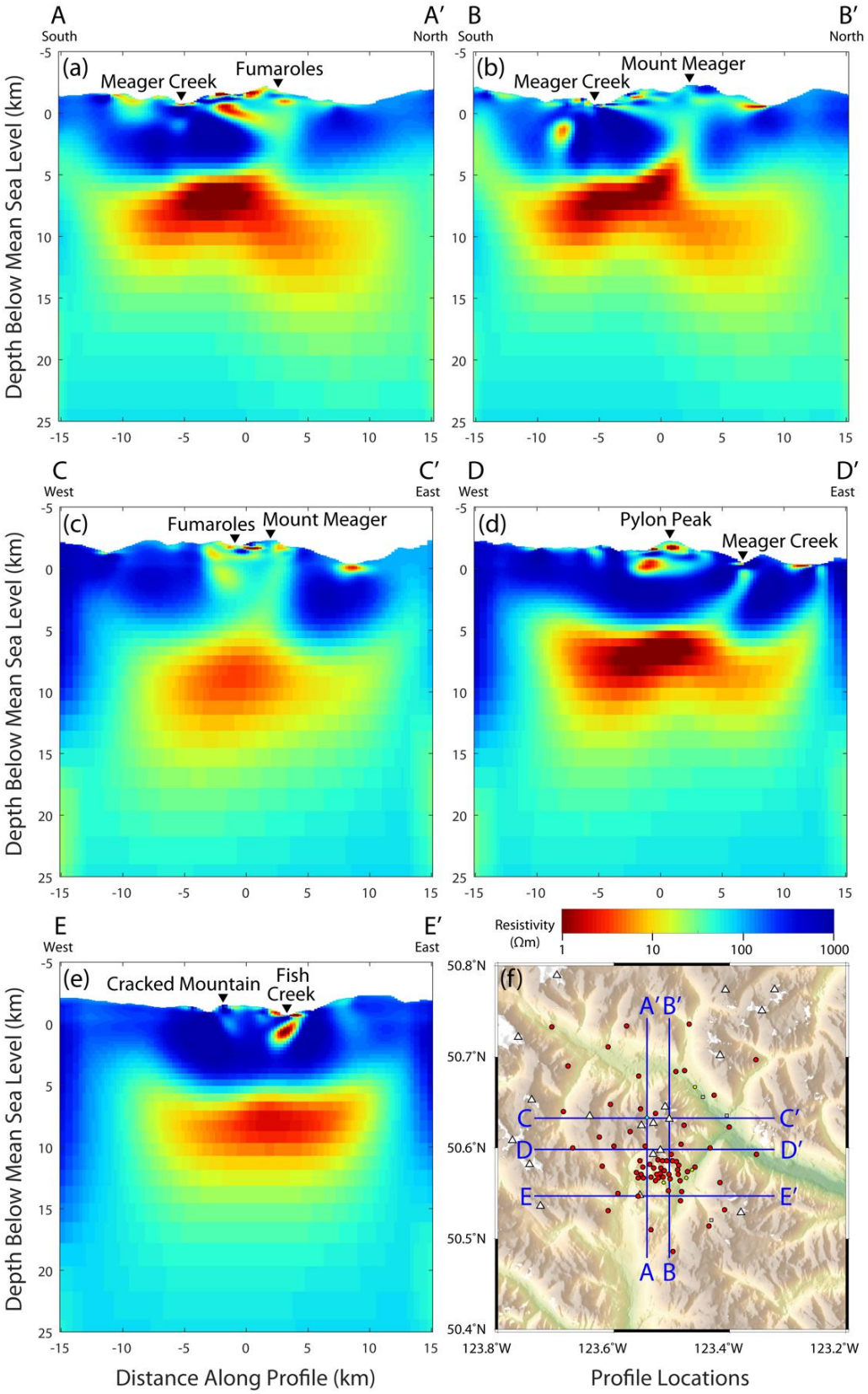


Figure 8. (a-e) Vertical slices of the preferred 3-D resistivity model. Black triangles indicate landmarks at the surface. (f) Topographic map with profile locations. (Hanneson and Unsworth, 2023)

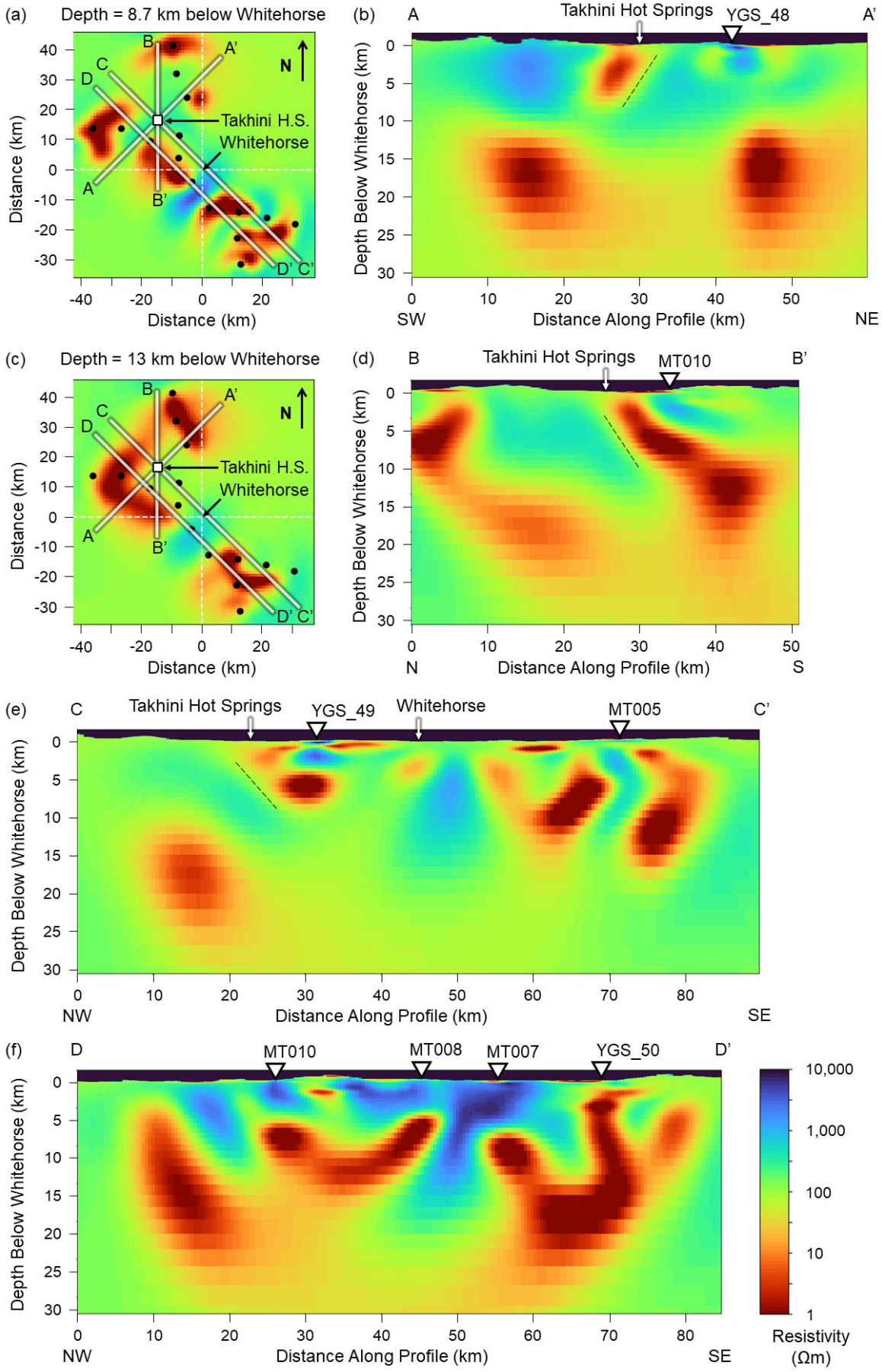


Figure 9. Slices of the preferred 3-D resistivity model. (a,c) Horizontal slices showing the locations of the cross-sections. (b,d,e,f) Vertical slices with the surface locations of Takhini Hot Springs and Whitehorse. The black region at the top of the cross-sections is the highly resistive atmosphere.

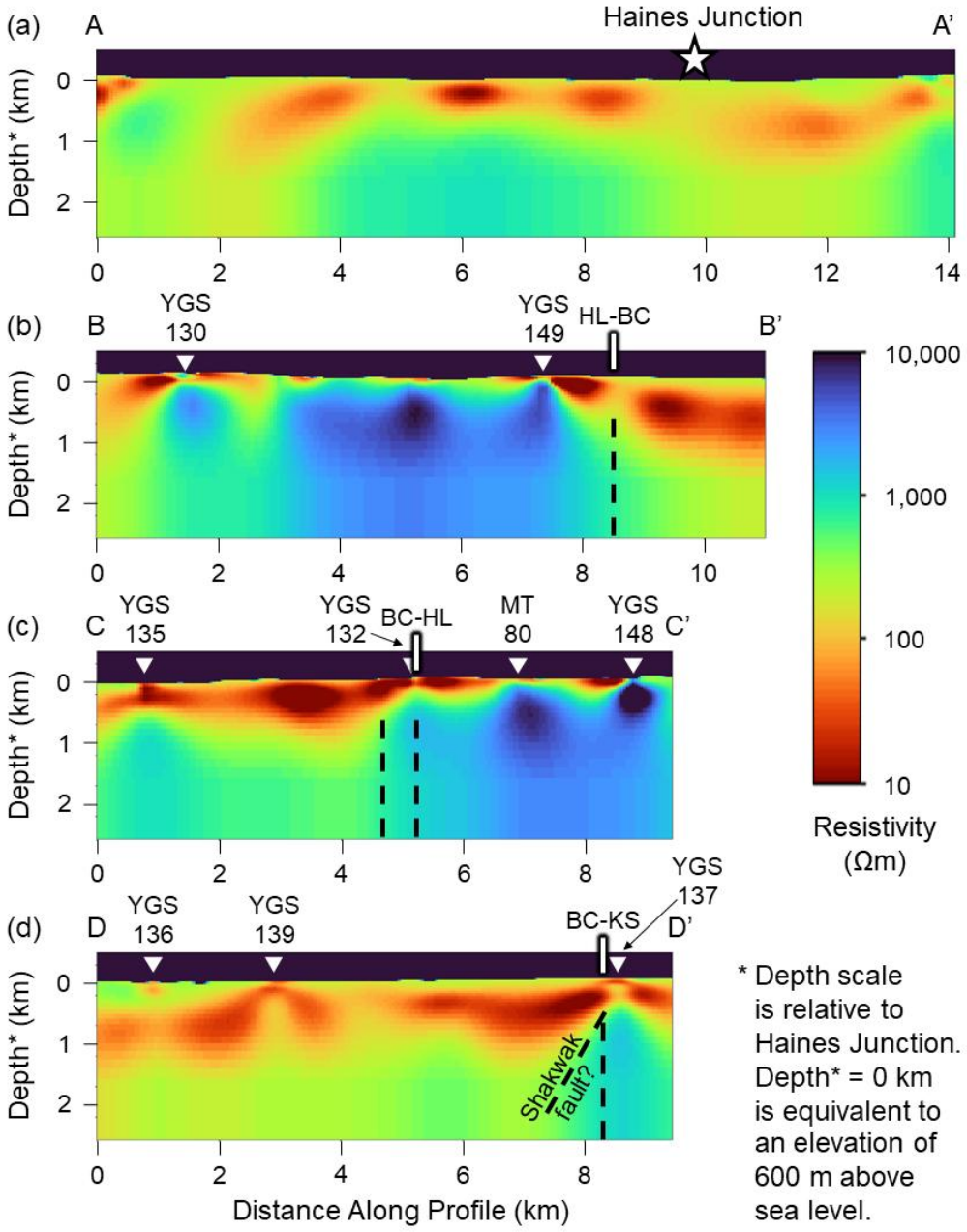


Figure 10. Vertical slices of the preferred 3-D resistivity model. Profile locations are shown in Figure 4. A-A' and B-B' are subparallel to the Shakwak fault. C-C' and D-D' are subperpendicular to the Shakwak fault. White triangles indicate locations of MT sites. BC = Bear Creek assemblage, HL = Hayden Lake suite, and KS = Kluane Schist. The black region at the top of the cross-sections is the highly resistive atmosphere.

The MT method is a valuable tool in geothermal exploration and research. The higher frequencies used in AMT facilitate the imaging of near surface geothermal systems in relatively high resolution, while the lower frequencies used in BBMT allow the imaging of crustal-scale systems including deep faults and magmatic systems. Western Canada has significant geothermal resources, both volcanic (e.g., the GVB) and fault-hosted (in various parts of the Canadian Cordillera). Canada is well-positioned to exploit these resources for clean, renewable heat and baseload power. The MT method has been, and will continue to be, a key component of exploration programs aiming to image and characterize these geothermal systems.

Acknowledgements

Funding was provided by NSERC, Future Energy Systems, Natural Resources Canada, Geoscience BC, and the Yukon Geological Survey.

REFERENCES

Colpron, M., Israel, S., Murphy, D., Pigage, L., and Moynihan, D.: Yukon bedrock geology map, *Yukon Geological Survey*, **Open File 2016-1**, (2016), 1:1,000,000 scale map and legend.

EBA Engineering Consultants Ltd.: Resource assessment for heat potential study, Haines Junction, YT, submitted to *Lessoway Moir and Partners*, **Project No. 1240049**, (2003), 76 p.

Gabrielse, H., Monger, J.W.H., Wheeler, J.O., Yorath, C.J., Carter, E.S., Orchard, M.J., Ross, C.A., Ross, J.R.P., Smith, P.L., Tipper, H.W., Sweeney, J.F., Stephenson, R.A., Currie, R.G., and DeLaurier, J. M.: Tectonic framework, *Geological Survey of Canada*, **Geology of the Cordilleran Orogen in Canada**, (1991), 15–59.

Ghomshei, M.M.: Canadian Geothermal Power Prospects, *Proceedings*, World Geothermal Congress 2010, Bali, Indonesia, (2010), 5 p.

Grasby, S.E., Allen, D.M., Bell, S., Chen, Z., Ferguson, G., Jessop, A., Kelman, M., Ko, M., Majorowicz, J., Moore, M., Raymond, J., and Therrien, R.: Geothermal energy resource potential of Canada, *Geological Survey of Canada*, **Open File 6914**, (2012), 322 p.

Hanneson, C., and Unsworth, M.J.: Magnetotelluric imaging of the magmatic and geothermal systems beneath Mount Meager, southwestern Canada, *Canadian Journal of Earth Sciences*, **60**, (2023), 1385–1403.

Harris, M.A., Russell, J.K., Barendregt, R., Porritt, L.A., and Wilson, A.: Explosive glaciovolcanism at Cracked Mountain Volcano, Garibaldi Volcanic Belt, Canada, *Journal of Volcanology and Geothermal Research*, **423**, (2022), 107477.

Hickson, C.J.: Character of volcanism, volcanic hazards, and risk, northern end of the Cascade magmatic arc, British Columbia and Washington State, *Bulletin of the Geological Survey of Canada*, **481**, (1994), 231–250.

Hormozzade Ghalati, F., Craven, J.A., Motazedian, D., Grasby, S.E., and Tschirhart, V.: Modeling a fractured geothermal reservoir using 3-D AMT data inversion: insights from Garibaldi Volcanic Belt, British Columbia, Canada, *Geothermics*, **105**, (2022), 102528.

Israel, S., Colpron, M., Cubley, J., Moynihan, D., Murphy, D.C., and Relf, C.: The Bear Creek assemblage: A latest Triassic volcano-sedimentary succession in southwest Yukon, *Yukon Geological Survey*, **Yukon Exploration and Geology 2014**, (2015), 99–112.

Israel, S., Murphy, D., Bennett, V., Mortensen, J., and Crowley, J.: New insights into the geology and mineral potential of the Coast Belt in southwestern Yukon, *Yukon Geological Survey*, **Yukon Exploration and Geology 2010**, (2011), 101–123.

Kelbert, A., Meqbel, N., Egbert, G.D., and Tandon, K.: ModEM: A modular system for inversion of electromagnetic geophysical data, *Computers & Geosciences*, **66**, (2014), 40–53.

Muñoz, G.: Exploring for Geothermal Resources with Electromagnetic Methods, *Surveys in Geophysics*, **35(1)**, (2014), 101–122.

Read, P.B.: Mount Meager Complex, Garibaldi Belt, Southwestern British Columbia, *Geoscience Canada*, **17(3)**, (1990), 167–170.

Russell, J.K., Stewart, M., Wilson, A., and Williams-Jones, G.: Eruption of Mount Meager, British Columbia, during the early Fraser glaciation, *Canadian Journal of Earth Sciences*, **58**, (2021), 1146–1154.

Stasiuk, M.V., Russell, J.K., and Hickson, C.J.: Distribution, nature, and origins of the 2400 BP eruption products of Mount Meager, British Columbia: Linkages between magma chemistry and eruption behaviour, *Bulletin of the Geological Survey of Canada*, **486**, (1996), 1–27.

Venugopal, S., Moune, S., Williams-Jones, G., Druitt, T., Vigouroux, N., Wilson, A., and Russell, J.K.: Two distinct mantle sources beneath the Garibaldi Volcanic Belt: insight from olivine-hosted melt inclusions, *Chemical Geology*, **532**, (2020), 119346.

Witter, J.B.: Analysis of geoscience data for geothermal exploration in the Whitehorse area, Yukon, *Yukon Geological Survey*, **Open File 2025-8**, (2025), 53 p.

Yukon Geological Survey: Yukon Digital Bedrock Geology, *Yukon Geological Survey*, (2024), https://data.geology.gov.yk.ca/Compilation/3 [accessed February 5, 2024].